PLASTIC DEFORMATION OF ALUMINUM BONDING WIRE IMPRESSED BY WEDGE BONDING TOOL

Vladimír Košel[1, 2], Javad Zarbakhsh[2], Michael Glavanovics[2]

[1]Slovak University of Technology in Bratislava, Faculty of Electrical Engineering and Information Technology,
81219 Bratislava, Ilkovičova 3, Slovakia
[2]KAI - Kompetenzzentrum Automobil- und Industrie- Elektronik GmbH
Europastrasse 8, A-9524 Villach, Austria

vladimir.kosel@k-ai.at (Vladimír Košel)

Abstract

Plastic deformation of aluminum bonding wires during the bonding process is investigated using the Finite Element Method (FEM) and compared to experimental results. The analysis is focused on the wedge bonding process of 250μm diameter aluminum wire. This study is performed on a three-dimensional (3D) FEM model using ANSYS, which includes the bonding wire, bonding tool and the underneath bonding pad. In the simulation setup, high emphasis is put on the wire modeling, however the bonding tool and the underneath pad are simplified. The overall geometry has a quarter dihedral symmetry which leads to reduced simulation time. The bonding tool is made up of carbide material, which is very stiff and therefore is considered as a rigid body. The considered material properties include the available plastic behavior for aluminum. In order to simulate the bonding process, a displacement constraint is applied to the bonding tool. The change of the bonding wire shape, the material displacements in the wire, and the distribution of plastic strain were investigated. The simulation results agree well with the experiments. The results of current study help us toward further understanding in reliability of power semiconductor products. They are also to be used in further thermo-mechanical simulations of power semiconductors.

Keywords: FEM, bonding process, aluminum wedge, plasticity

Presenting Author's biography

Vladimír Košel. 2003 graduated in electrical engineering at Slovak University of Technology (STU) in Bratislava. He started his PhD in 2003 at STU, and worked on reliability of Smart Power Switches at Infineon Technologies in Villach, Austria. Since 2006, he is continuing his PhD project at Kompetenzzentrum Automobil- und Industrie-Elektronik in Villach, Austria

ISBN 978-3-901608-32-2

Copyright © 2007 EUROSIM / SLOSIM

1 Introduction

Wire bonding is a favorite technique in power semiconductors for electrical connections between pads of power structures and the package pins [1, 2]. In the wire-bonding process the wire is used to establish the electrical connection between the semiconductor chip and the external device leads. Depending on application and cost of a product, different materials and bonding methods are used for wire connections [3]. Aluminum wires are preferred to gold or copper ones, due to their low cost, simple handling, and good electrical and mechanical properties [4, 5]. The wire size must be compatible with the semiconductor pad area, therefore wires with diameters in the range of 15 μm to 250 μm or even more are used in high power applications. There are basically two forms of wire bonding technique, the ball bond and wedge bond [6].

Power semiconductors are primarily used to control the flow of energy between the energy source and the load, with great precision, with extremely fast control times and with low dissipated power. The application of IC technologies on power semiconductor devices has resulted in advanced, self-protecting components with low power dissipation, simple drive characteristics, good control dynamics, together with a direct interface to the microelectronics [7].

The trend of chip cost reduction leads to chip size shrinkage and thus to higher power dissipation density on the chip [7-9]. The consequence is higher thermal and mechanical stress [10]. Continuous operation of semiconductors under electrical and thermal overload conditions leads to degradation and subsequently to device failure. Under the high stress circumstances the bonding wires are subjected to extreme operating conditions which have impact on the reliability of the whole semiconductor device [11, 12]. Very often the failure mechanism is an electrical and mechanical degradation of the bonding interface – the interface between the pad and bonding wire. In many cases the reliability of a semiconductor device is reduced, due to the not optimized bonding process. Cratering and heel crack are well-known defects resulting from a wrong bonding process [5, 13-15]. The cratering problem is often referred to the severe damage in semiconductor pad, which is due to overbonding. The heel cracks can be caused by using a sharp bonding tool or due to the vibration just before and during the fast bonding tool lift-up [3].

There are many parameters like shape of bonding tool, wire diameter, acting force, ultrasonic energy, mechanical properties and many others, which influence the quality of the bonding interface [2, 16]. A study of each parameter usually reveals a relationship between the material, the bounding setup, and stress distribution. To troubleshoot the mechanical problems in wire bonding, one should fully understand the material behavior and the deformation of the bounding wire.

In this study the plastic deformation of a 250 μm diameter aluminum wire during wedge bonding process is investigated. Wires of this diameter are often used in smart power semiconductors. The shape change of the aluminum wire due to plastic deformation during the bonding process as well as a material displacement inside the wire is studied. Additionally, the bonding contact formation between a pad and aluminum wire is observed. The result of this work helps toward better understanding of the wedge bonding process of aluminum wires and design rules for optimization of the process.

2 Simulation model

The schematic view of the bonding setup is shown in Fig. 1. In reality, the whole setup consists of die, pad, wire and bonding tool. The bonding setup possesses the quarter dihedral symmetry which allows us to model only one quarter of the setup. The meshed FEM model is depicted in Fig. 2. For simplicity, the substrate is not included in the simulation setup. The simulation model of this setup was built with a so called “bottom-up” approach in ANSYS. In this approach, at first the keypoints are created, then using those keypoints the higher-order solid model entities (that is, lines, areas, and volumes) will be created.

The bonding wire (Fig. 1 structure 3) is created by several cylinders with different thickness. The cylinder thickness increases exponentially in x-axis outwards from the bonding tool edge as depicted in Fig. 3. In this region high plastic deformations are expected. The adjacent cylinders are connected together by gluing. The round part of cylinders is built by spline-based areas. This complex modeling approach has several advantages. The meshing algorithm is explicitly forced to create a finer mesh around the bonding tool edge. In addition, the cylinders can be individually selected and unselected which can be used for advanced post-processing.

The bonding wire is made of aluminum. The material properties of aluminum are modeled by a Bilinear Isotropic Hardening (BISO) material model [17] which considers plastic behavior of materials.

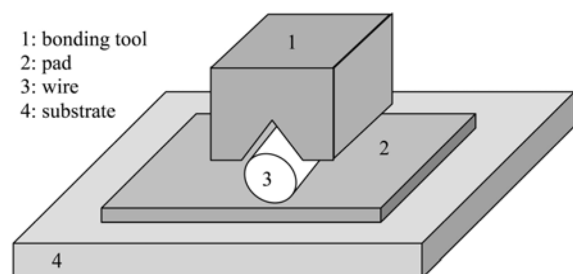

Fig. 1 Schematic view of bonding setup

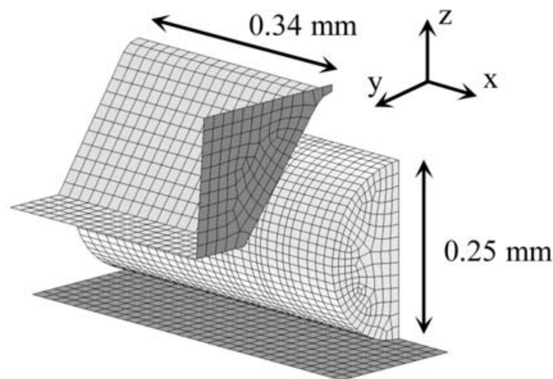

Fig. 2 FEM model of bonding setup which is meshed by rectangular plane and hexahedral solid elements

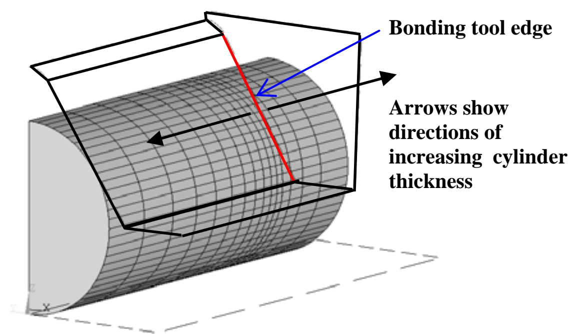

Fig. 3 Geometrical model of bonding wire consisting of several cylinders

Fig. 4 Wedge bonding tool

Fig. 4 shows the real bonding tool, which consists of V-shaped wedge plates and adjacent horizontal side-plates. The considered bonding tool is made of carbide based material, which is much stiffer than aluminum. Due to this fact, the bonding tool is considered as an ideally stiff body. This allows us to model the bonding tool by the rigid areas modeling technique. In the FEM model, only those areas are considered which are assumed to touch an area of bonding wire during the bonding process. This way the number of elements in the FEM model is greatly reduced.

The material stiffness and the yield stress of the aluminum wire are much lower than those of the thin aluminum pad, and underneath silicon substrate. Therefore, for simplicity, the pad (Fig. 1 structure 2) was modeled by a rigid area as well.

In the bonding process the bonding tool presses onto the wire. From the other side the wire is constrained by the pad. To transfer forces between pad, wire and the bonding tool, contact elements are used. Because the surface of aluminum wire has a certain roughness, the friction coefficient was defined for aluminum.

During the bonding process, the pressure transmitted from the bonding tool to the wire is large enough to cause plastic deformations. There are two possibilities to simulate the deformation of the wire by the bonding tool; either by a displacement constraint or by force acting in vertical direction on the bonding tool. In this paper the first possibility is used. The final position of the bonding tool in z direction was measured and used as a bonding tool constraint.

3 Results and discussions

The deformation evolution of an aluminum bond wire is obtained during the bonding process, as it is shown in Fig. 5.

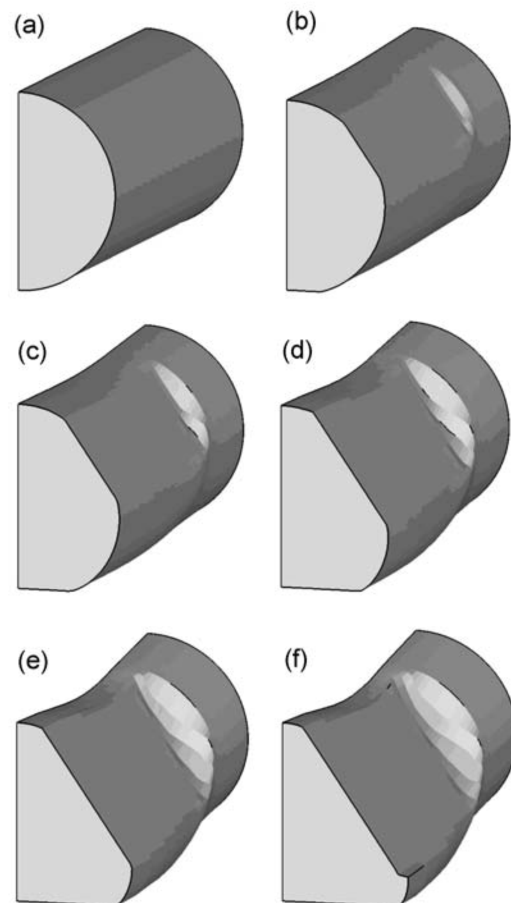

Fig. 5 Sequence of wire deformation during bonding process

Due to the plastic deformation of the aluminum wire, and existing friction among contact elements, parts of the wire reshape immediately after the start of the bonding process, while the uppermost part has not yet contact to the V-shaped plates (Fig. 5b), and therefore

 Copyright © 2007 EUROSIM / SLOSIM

stays unchanged. Later, in Fig. 5c-e, the lower part of the wire takes the shape of the pad and lays down on it. As the bonding tool moves further down, there is not enough space left beneath the V-shaped plates, and therefore material is squeezed out to the horizontal side-plates, as it is shown in Fig. 5f. The free ending of the wire is also bent upward as a result of plastic deformation and squeezed along the x-axis.

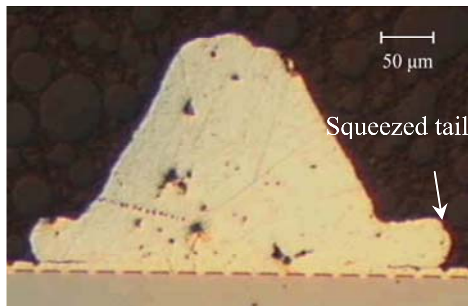

Fig. 6 Cross-section of real bond wire

To verify the simulation results, a mechanical cross-section of a real power semiconductor product bonded by 250 μm diameter aluminum wire is made through an aluminum bond wire, shown in Fig. 7. The simulation result fits well with the real cross-section. The squeezed tail of the wire, which is laid on the pad along y-axis, is not symmetric in the experiment, however the length of the real squeezed tails and their shapes are well comparable to those of simulation.

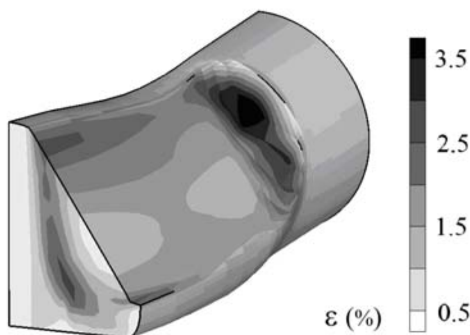

Fig. 7 Contour plots of von Mises plastic strain after bonding process

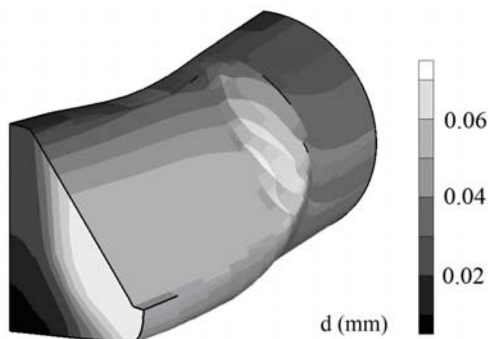

Fig. 8 Contour plots of magnitude of displacement, after bonding process

Fig. 7 shows the contour plot of von Mises plastic strain [18]. It shows that the middle part of the simulation volume has very high strain. The overall maximum strain of 3.5% happens near the edge of the V-shaped plates.

The contour plot of displacement magnitude is shown in Fig. 8. The lowest part of the wire, which was laid on the pad does not change its place, while the maximum of 60 μm displacement, happens in the squeezed tail.

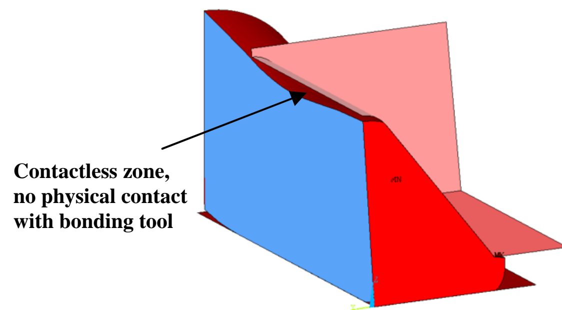

Fig. 9 Wire deformation after bonding process, the bonding tool in final position

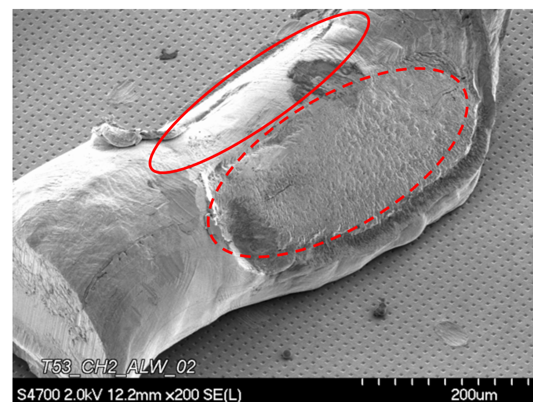

Fig. 10 SEM image of 250μm aluminum wire after bonding process, solid line region: contactless zone, low surface roughness; dash line regions: touch with bonding tool, high surface roughness

Fig. 9 shows the deformation of the wire after the bonding process along with the bonding tool in final bonding position. The simulation result shows that the V-shaped plates have no physical contact with the most upper wire surface along the entire x-axis. This is also valid for earlier sequences of the bonding process. In order to verify this result with reality a SEM image of several real aluminum wires was taken (example in Fig. 10). In the image, regions with low and high surface roughness can be distinguished. The most upper surface on the wire has the same roughness as the other parts of the wire which are not involved in the bonding process. This implies that the most upper surface of the wire had no touch with the V-shaped plates of the bonding tool.

 Copyright © 2007 EUROSIM / SLOSIM

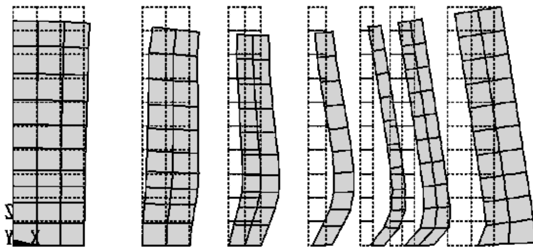

Fig. 11 Resulting deformation of cylinders in XZ symmetry plane

The aluminum displacement in the wire is also investigated. Fig. 11 shows the deformation of several selected cylinders in XZ symmetry plane and their original shape and position. Due to the friction which was defined for aluminum, material near the pad sticks to some extends to the pad. The consequence is that the cylinders near the bonding tool edge are highly deformed in their lower part.

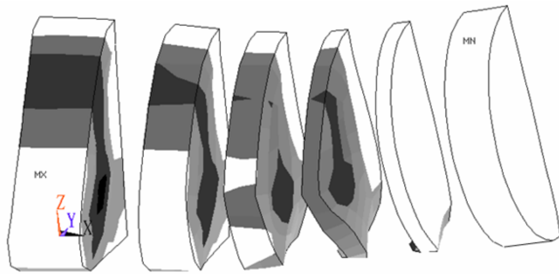

Fig. 12 Plastic strain intensity in selected cylinders (dark colors show high intensity)

In Fig. 12 it can be seen that the high plastic strain occurs in the middle of the simulated volume starting at the YZ symmetry plane and continuing along the x-axis till the bonding tool edge. Immediately beyond the bonding tool edge the strain rapidly decreases.

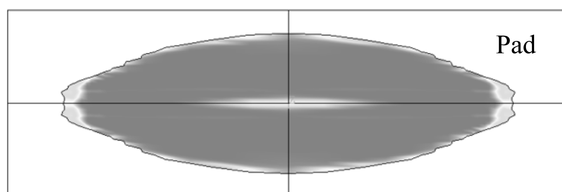

Fig. 13 Top view of the resulting contact area between pad and the aluminum wire (shown as quarter dihedral symmetry expansion)

In addition, the contact area between the pad and the deformed wire was investigated. Based on our measurements, the thickness of the wire to pad interface created during the ultrasonic process is as low as 1 µm. The simulation result in Fig. 13 shows a cross-section of the wire which is made 500 nm over the pad.

The resulting contact area in Fig. 13 has an elliptical shape which is also reported in some experimental works on wedge bonding (Fig. 14a and b). Fig. 13 shows that the von Mises stress is not uniformly distributed over the bonding contact area. It is also shown that the middle part of the contact area has lower stress in comparison to the outer parts. In previously reported experimental observations [3, 19], it has been shown that at the center area, the wire-to-pad contact is either weakly welded or stayed unwelded (Fig. 14c). We believe that the quality of the welding might be related to the interfacial stress during or after the bonding process. In reality, one can easily remove or partially lift up the wire, so that the welding patterns can be seen. The center usually remains unwelded [3].

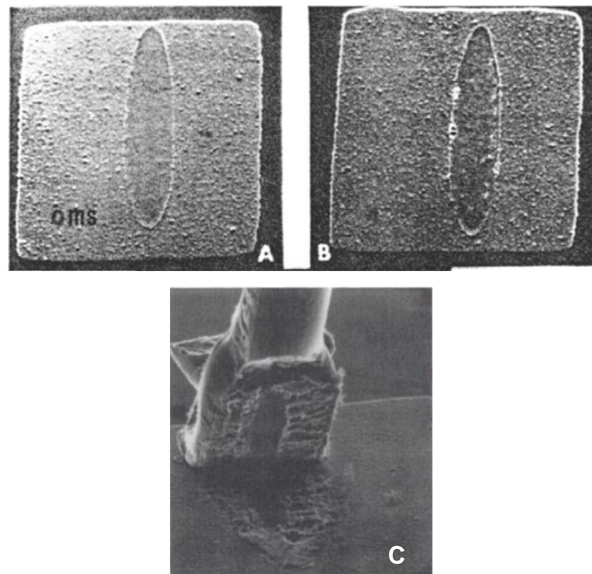

Fig. 14 a,b.) Pattern of typical bonding area after wedge bond lift-off. c) the center of the bonding wire has weak contact the pad and stays unwelded. Follow [3]

4 Conclusion

The plastic deformation of an aluminum bond wire during the wedge bonding process is analyzed using 3D FEM simulation, and compared to the experiments. It is shown that during the bonding process, the material of wire experiences large plastic strain and is squeezed out of the bonding tool. The plastic strain has a dominant effect in the middle of the simulated quarter wire, whereas the wire part beyond the bonding tool experiences low stress. The maximum plastic strain occurs underneath the bonding tool edge.

Based on the wire surface roughness observations, it is shown that the most upper surface of the wire has no touch with the V-shaped plates of the bonding tool, which was also observed in the simulations.

It is also shown that the middle part of the contact area has lower stress in comparison to the outer parts, which might correspond to experimental observations

reporting either weakly welded or unwelded contact at the center area of the wire-to-pad interface.

Further investigations should be also done to improve contact formation during the bonding process and thus to enhance the reliability of power semiconductor products. The knowledge of the current study will be used for further thermo-mechanical simulations and investigations of power semiconductor devices.

5 Acknowledgement

This work was jointly funded by the Federal Ministry of Economics and Labour of the Republic of Austria (contract 98.362/0112-C1/10/2005) and the Carinthian Economic Promotion Fund (KWF) (contract 98.362/0112-C1/10/2005).

The authors would like to thank J. Maerz, M. Stecher, T. Smorodin, Ch. Bohm, P. Nelle, G. Kravchenko and E. Orejola from Infineon Technologies AG in Munich for providing us with information on bonding process and material properties. We also thank our colleagues S. Hainz and A. Satz in KAI GmbH for their valuable discussions, and thank M. Hanke from CADFEM in Berlin for technical ANSYS support.

6 References

[1] Kraus, R. and H.J. Mattausch, *Status and trends of power semiconductor device models for circuit simulation.* Ieee Transactions on Power Electronics, 1998. **13**(3): p. 452-465.

[2] Perfecto, E.D., et al., *Evolution of engineering change and repair technology in high performance multichip modules at IBM.* Ieee Transactions on Advanced Packaging, 1999. **22**(2): p. 129-135.

[3] Harman, G.G., *Wire Bonding in Microelectronics: Materials, Processes, Reliability, and Yield*. 1997: McGraw-Hill Professional.

[4] Greving, D.J., J.R. Shadley, and E.F. Rybicki, *Effects of Coating Thickness and Residual-Stresses on the Bond Strength of Astm C633-79 Thermal Spray Coating Test Specimens.* Journal of Thermal Spray Technology, 1994. **3**(4): p. 371-378.

[5] Ramminger, S., N. Seliger, and G. Wachutka, *Reliability model for Al wire bonds subjected to heel crack failures.* Microelectronics Reliability, 2000. **40**(8-10): p. 1521-1525.

[6] Yeh, C.L., Y.S. Lai, and C.L. Kao, *Transient simulation of wire pull test on Cu/low-K wafers.* Ieee Transactions on Advanced Packaging, 2006. **29**(3): p. 631-638.

[7] Lorenz, L. and H. Mitlehner, - *Key power semiconductor device concepts for the next decade.* 2002. **- 1**(-): p. - 569 vol.1.

[8] Murphy, B.T., *Cost-size optima of monolithic integrated circuits*. 1964. p. 1537-1545.

[9] Lee, C.C., et al., *Solder joints layout design and reliability enhancements of wafer level packaging using response surface methodology.* Microelectronics Reliability, 2007. **47**(2-3): p. 196-204.

[10] Glavanovics, M. and H. Zitta, *Dynamic hot spot temperature sensing in smart power switches*, in *28th European Solid-State Circuits Conference (ESSCIRC 2002)*. 2002: Florence, Italy. p. - 298.

[11] Detzel, T., M. Glavanovics, and K. Weber, *Analysis of wire bond and metallization degradation mechanisms in DMOS power transistors stressed under thermal overload conditions.* Microelectronics Reliability, 2004. **44**(9-11): p. 1485-1490.

[12] Glavanovics, M., T. Detzel, and K. Weber, *Impact of thermal overload operation on wirebond and metallization reliability in smart power devices*, in *Essderc 2004: Proceedings of the 34th European Solid-State Device Research Conference*, R.P. Mertens and C.L. Claeys, Editors. 2004, Ieee: New York. p. 273-276.

[13] Tan, C.W. and A.R. Daud, *Bond pad cratering study by reliability tests.* Journal of Materials Science-Materials in Electronics, 2002. **13**(5): p. 309-314.

[14] Joshi, K.C., *Formation of Ultrasonic Bonds between Metals - Is Based on Dislocation Processes Which Are Manifested as a Unique Softening Phenomenon.* Welding Journal, 1971. **50**(12): p. 840-&.

[15] Tan, C.M. and Z.G.B. Gan, *Failure mechanisms of aluminum bondpad peeling during thermosonic bonding.* Ieee Transactions on Device and Materials Reliability, 2003. **3**(2): p. 44-50.

[16] Hsia, C.C., *The quest of porous ELK materials for high performance logic technologies.* Microelectronic Engineering, 2006. **83**(11-12): p. 2055-2058.

[17] Chaboche, J.L., *On Some Modifications of Kinematic Hardening to Improve the Description of Ratchetting Effects.* International Journal of Plasticity, 1991. **7**(7): p. 661-678.

[18] Anderson, T.L., *Fracture Mechanics: fundamentals and applications*. 1995: CRC Press.

[19] Ding, Y., J.K. Kim, and P. Tong, *Effects of bonding force on contact pressure and frictional energy in wire bonding.* Microelectronics Reliability, 2006. **46**(7): p. 1101-1112.

ISBN 978-3-901608-32-2 *Copyright © 2007 EUROSIM / SLOSIM*